

## Magnetic permeability of sputtered permalloy thin films

This article has been downloaded from IOPscience. Please scroll down to see the full text article.

1993 J. Phys.: Condens. Matter 5 1257

(<http://iopscience.iop.org/0953-8984/5/9/010>)

View [the table of contents for this issue](#), or go to the [journal homepage](#) for more

Download details:

IP Address: 171.66.16.159

The article was downloaded on 12/05/2010 at 13:00

Please note that [terms and conditions apply](#).

## Magnetic permeability of sputtered permalloy thin films

D Dimitrov, I Halianov, J Kassabov and S Marinov

Institute of Solid State Physics, Bulgarian Academy of Sciences, 72 Tzar Chausse, 1784-Sofia, Bulgaria

Received 14 April 1992, in final form 4 January 1993

**Abstract.** The magnetic permeability of sputtered permalloy thin layers has been investigated by a specially designed experimental set-up. The investigation shows that the magnetic permeability depends strongly on the argon pressure during deposition. Higher permeability of the sputtered layers is obtained for argon at pressure less than  $5 \times 10^{-2}$  mbar.

### 1. Introduction

Recently, interest in thin, high permeability magnetic layers has increased. This is due mainly to possible applications in integrated thin layers, magnetic heads and in small size magnetic sensors [1–5]. The application of thin, high permeability magnetic layers as a part of magnetic sensors relies mainly on the variation of the magnetic permeability in proportion to the applied external magnetic field. This variation is connected with the coercivity, composition, thickness and shape of the layers and also depends on the technological conditions of sample preparation [6–10].

In this study we have examined the properties of a thin ( $\approx 1000 \text{ \AA}$ ) permalloy layer obtained by RF magnetron sputtering. The effect of argon pressure and power density of the deposition process on the magnetic permeability of the layers has been investigated.

### 2. Experimental technique and sample preparation

#### 2.1. Sample preparation

The films used were prepared by RF magnetron sputtering in a Leybold–Heraeus system Z-400. This is a turbo-molecular pumped system with a base pressure of the order of  $10^{-6}$  mbar.

The layers were deposited on thermally oxidized silicon wafers. The substrates were cleaned in  $\text{H}_2\text{O}_2:\text{H}_2\text{SO}_4 = 1 : 2$  solution and then rinsed in deionized water. Prior to deposition, an ion bombardment was used for final cleaning of the substrates. No heating was applied to the substrate during deposition. However, it was possible that the substrate temperature might increase to  $100^\circ\text{C}$  due to substrate contact with the plasma components. No external magnetic field was applied to the growing layer, since this is very difficult to achieve in a Z-400 system. The layers obtained, therefore, had random orientation of the easy axis of magnetization. In order to obtain reproducible orientation of the easy axis of magnetization all samples were annealed after the deposition. The annealing was performed in two steps: (i) annealing the samples in  $\text{H}_2$  atmosphere at

450 °C for 15 min which reduced the number of defects introduced during the deposition; (ii) cooling the samples in a H<sub>2</sub> atmosphere with an external homogeneous magnetic field ≈ 100 Oe applied to the plane of the samples.

The experimental samples obtained by different deposition conditions are summarized in the table 1.

Table 1. Technological conditions for sample preparation.  $V_g$  deposition rate,  $d$  = layer thickness.

Power density (W cm <sup>-2</sup> )	$P_{Ar}$ (mbar)			
	$1 \times 10^{-1}$	$5 \times 10^{-2}$	$1 \times 10^{-2}$	$5 \times 10^{-3}$
$P_{RF} = 2.3$ ( $U_{RF} = 1$ kV) $I_c = 100$ mA)	Samples 2 $V_g = 20 \text{ \AA min}^{-1}$ $d = 1000 \text{ \AA}$	Samples 8 $V_g = 45 \text{ \AA min}^{-1}$ $d = 1350 \text{ \AA}$	Samples 14 $V_g = 63 \text{ \AA min}^{-1}$ $d = 1260 \text{ \AA}$	Samples 20 $V_g = 56 \text{ \AA min}^{-1}$ $d = 1120 \text{ \AA}$
	$P_{RF} = 4.75$ $U_{RF} = 1.5$ kV $I_c = 140$ mA	Samples 4 $V_g = 69 \text{ \AA min}^{-1}$ $d = 1411 \text{ \AA}$	Samples 10 $V_g = 145 \text{ \AA min}^{-1}$ $d = 1450 \text{ \AA}$	Samples 16 $V_g = 240 \text{ \AA min}^{-1}$ $d = 1200 \text{ \AA}$
$P_{RF} = 7.7$ $U_{RF} = 2$ kV $I_c = 170$ mA)	Samples 6 $V_g = 137 \text{ \AA min}^{-1}$ $d = 1370 \text{ \AA}$	Samples 12 $V_g = 352 \text{ \AA min}^{-1}$ $d = 1408 \text{ \AA}$	Samples 18 $V_g = 550 \text{ \AA min}^{-1}$ $d = 1100 \text{ \AA}$	Samples 24 $V_g = 561 \text{ \AA min}^{-1}$ $d = 1122 \text{ \AA}$

## 2.2. Characterization of layers

The experimental set-up used for measurement of magnetic bias dependence of magnetic permeability of permalloy layers is schematically shown in figure 1. It consists of a signal generator, a specially designed bridge circuit and a lock-in amplifier which detects the voltage drop upon test inductance  $L$ . The signal from the lock-in amplifier is recorded by an  $X$ - $Y$  recorder versus the external test bias magnetic field. The principle of measurements of the magnetic permeability is based on the change in the magnetic inductance  $L$  of the exiting test coil due to the presence of the magnetic core. The resulting inductance  $L_c$  of the coil is:

$$L_c = k\mu L$$

where  $\mu$  is the magnetic permeability of the core, and  $k$  is a proportional constant. The constant  $k$  depends on the shape of the core in the exiting coil, on the homogeneities of the magnetic field created by the exiting coil and on the frequency at which the measurements were carried out. Specially calibrated samples have been used to determine the precise value of  $k$ .

To obtain a homogeneous AC magnetic field throughout the investigated sample, the exiting coil should have large volume and, therefore, a large inductance (of the order of 20  $\mu$ H). This inductance reduces the signal created by the measured sample. A special balance coil, identical to the exiting coil, is added to form a bridge circuit in order to increase sensitivity (see figure 1). The signal from the bridge circuit, proportional to variation of magnetic permeability of the sample, is amplified by the lock-in amplifier (PAR Model 128A) and recorded by an  $X$ - $Y$  recorder. The external magnetic bias field is created by an independent external electronic circuit which ensures a homogeneous

magnetic field. The bias magnetic field ramp-rate during measurements is of the order of  $0.1 \text{ Oe s}^{-1}$ . This low ramp-rate allowed analysis of the peculiarities in the  $\mu$  versus  $H_{\text{ext}}$  curves. These peculiarities are due to dispersion of the magnetization of the samples.

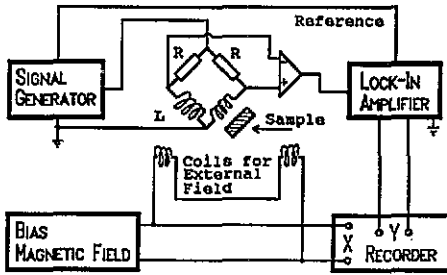


Figure 1. Schematic representation of the experimental set-up for permeability measurements.

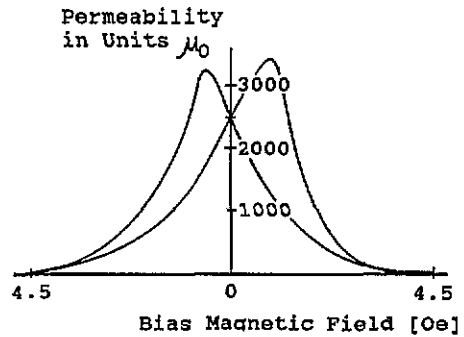


Figure 2. Typical dependence of  $\mu$  on DC magnetic bias.

In figure 2 the typical curve of dependence of the magnetic permeability on the external magnetic field  $H_{\text{ext}}$  is shown (sample 16 of table 1). The two maxima of the magnetic permeability coincide well with the coercivity  $H_c$  of the sample measured by the standard  $B$ - $H$  meter.

### 3. Results and discussions

The samples shown on table 1 were measured to determine the effect of argon pressure on the magnetic bias dependence of the magnetic permeability. The measurement was carried out by the experimental set-up shown in figure 1. In order to avoid the geometrical shape of the layers affecting the measured magnetic permeability, all layers were patterned by photolithography.

The measured bias dependence of the magnetic permeability shows that the two permeability peaks (see figure 2) differ in their dependence on the orientation of the sample. The value of the measured permeability at zero bias field of a sample in the easy direction is greater than that in the hard direction. All data for magnetic permeability presented below are for a zero bias field in the hard axes of the samples. This means that the initial permeability of the samples is used for characterization.

Figure 3 shows the effect of power density on relative magnetic permeability of the sputtered layers. The different curves represent different constant values of argon pressure in the vacuum chamber. As can be seen from the figure, the dependence of the magnetic permeability of the layers on the sputtering power density is similar at both high and low argon pressures; the curves are almost parallel. Obviously this dependence is connected with the deposition rate of the layers. At constant pressure the deposition rate depends linearly on the sputtering power density of the deposition process.

However, as can also be seen from figure 4, the effect of the argon pressure in the reactor chamber is crucial for the magnetic permeability of the layers. A sharp drop in the magnetic permeability of the sputtered layer has been observed for argon pressures above  $5 \times 10^{-2}$  mbar. Presumably this effect is connected with impurities incorporated in the layers. Similar behaviour of the dependence of the

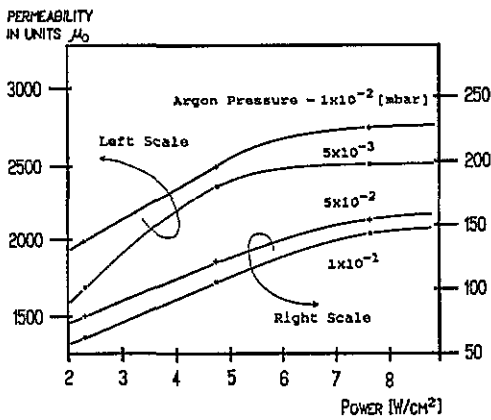


Figure 3. Dependence of the thin film permeability on the power density at constant Ar pressure.

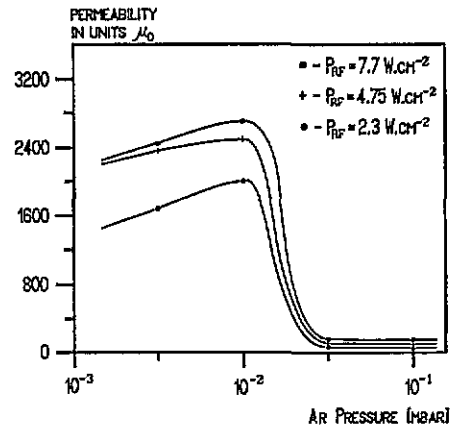


Figure 4. The effect of the Ar pressure on the magnetic permeability of the layers.

coercive force on the argon pressure has been observed in earlier investigations [6]. The coercive force of the layers sharply decreases with decreasing argon pressure and below  $5 \times 10^{-2}$  mbar becomes almost independent of the pressure.

#### 4. Conclusion

A permalloy thin layer of  $1000 \text{ \AA}$  thickness has been deposited on a silicon substrate by a magnetron sputtering system. The different layers have been obtained under different parameters of the sputtering process. The permeability of the layers has been measured by a specially designed experimental set-up. The investigation shows that the magnetic permeability depends strongly on the argon pressure during deposition. The high permeability layers are obtained at argon pressures less than  $5 \times 10^{-2}$  mbar.

#### Acknowledgments

We acknowledge the helpful discussion with Professor N Kirov.

#### References

- [1] Yamaguchi M, Hirai N, Kawasaki H and Ara K I 1990 *IEEE Trans. Magn.* MAG-26 1569
- [2] Garshelis J and Fiegel S 1990 *J. Appl. Phys.* 67 5580
- [3] Harada K, Sunouchi Y and Sakamoto H 1989 *IEEE Trans. Magn.* MAG-25 3399
- [4] Kobayashi T, Nakatani R, Ootomo S and Kamasaka N 1987 *IEEE Trans. Magn.* MAG-23 2746
- [5] Dimitrov D B 1993 *Sensors Actuators* at press
- [6] *Encyclopaedia of Semiconductor Technology* 1984 (New York: Wiley) p 479
- [7] Brouha M, van der Borst A J C, Turk G W and Witmer C H M 1986 *J. Magn. Magn. Mater.* 54-57 1665
- [8] Nishimura C, Nagai Y, Yanagisawa K and Toshima T 1987 *IEEE Trans. Magn.* MAG-23 2728
- [9] Takahashi M and Shimatsu T 1990 *IEEE Trans. Magn.* MAG-26 1485
- [10] Soohoo R 1965 *Magnetic Thin Films* (New York: Harper & Row)